Evaluation of a Correction Method for ^{111}In-Pentetreotide SPECT Imaging of Gastroenteropancreatic Neuroendocrine Tumors

Takao Kanzaki[1,2], Yasuyuki Takahashi[2], Tetsuya Higuchi[3], Xieyi Zhang[4], Nao Mogi[1], Takayuki Suto[1], and Yoshito Tsushima[3]

[1]Department of Radiology, Gunma University Hospital, Gunma, Japan; [2]Department of Nuclear Medicine Technology, Hirosaki University Graduate School of Health Sciences, Aomori, Japan; [3]Department of Diagnostic Radiology and Nuclear Medicine, Gunma University Graduate School of Medicine, Gunma, Japan; and [4]Laboratory of Biopharmaceutics, Department of Pharmacology, Faculty of Pharmacy, Takasaki University of Health and Welfare, Gunma, Japan

The number of patients with the extremely rare disease gastroenteropancreatic (GEP) neuroendocrine tumor (NET) has increased rapidly in recent years. ^{111}In-pentetreotide SPECT in somatostatin receptor scintigraphy has been used for the assessment of GEP NET patients. To diagnose GEP NET, appropriate selection of image correction parameters is critical. Correction methods may improve the ^{111}In-pentetreotide SPECT image quality, but there is currently no standard technique. The purpose of this study was to determine the optimal correction parameter settings for ^{111}In-pentetreotide SPECT. **Methods:** A phantom study produced images with a tumor-to-background ratio of as high as 16:1. A triple energy window was used for scatter correction (SC), and attenuation correction (AC) was CT-based. Correlation analysis was performed in 4 groups: no correction (NC), SC, AC, and combined SC with AC (CC). The ^{111}In-pentetreotide SPECT results for 20 randomly selected patients (13 men and 7 women; age range, 37–81 y) with confirmed GEP NET were analyzed using data collected 4 h after injection of 111 MBq of ^{111}In-pentetreotide. Emission data were reconstructed using ordered-subset expectation maximization (OSEM) with different settings. Different combinations of the correction parameters were used to analyze the contrast-to-noise ratios (CNRs) obtained with the phantom. In the clinical study, 20 GEP NET patients were used to evaluate the GEP NET lesion CNR by 4 different image correction methods obtained from ^{111}In-pentetreotide SPECT images: NC, SC, AC, and CC. NC was used as a reference method. **Results:** The phantom study revealed that the optimal energy window in the photopeak for somatostatin receptor scintigraphy was 171 keV ± 10% and 245 keV ± 7.5%, and the optimal OSEM reconstruction conditions were 8 subsets and 6 iterations. Among the OSEM collection conditions, CC produced a significantly higher CNR than NC or SC ($P < 0.05$). In the clinical study, CC was found to increase the CNR ($P < 0.05$). **Conclusion:** CC improves the correction in ^{111}In-pentetreotide SPECT studies, compared with NC, providing better contrast and sharper outlines of lesions and organs.

Key Words: somatostatin receptor scintigraphy; ^{111}In-pentetreotide; NET

J Nucl Med Technol 2020; 48:326–330
DOI: 10.2967/jnmt.120.249680

Neuroendocrine tumors (NETs) from neuroendocrine cells are rare, with a reported annual age-adjusted incidence of about 3–5/100,000 (*1,2*). Most of these tumors are derived from the gastroenteropancreatic system. However, in recent years, according to an epidemiologic survey conducted in Japan, the number of patients with NETs has increased rapidly (*3*). This increase may be due in part to improvements in imaging and biochemical methods of detection. As advanced clinical study results for NETs became recognized, a World Health Organization classification for gastroenteropancreatic (GEP) NETs was introduced, with a grading system based on the mitotic index and Ki-67 proliferation index (*4*). NET symptoms for diagnosis can be caused by hormonal excess, local tumor growth, metastatic spread (*5*), and high expression of several receptors (*6*).

Recent clinical studies have indicated that ^{111}In-pentetreotide SPECT in somatostatin receptor scintigraphy is effective for the diagnosis and staging of GEP NETs (*7*). In contrast, because of the small lesion size, the various anatomic locations, and the low metabolic rate, CT, ultrasound, and MRI are often insufficient for GEP NET diagnosis (*8*). Therefore, functional imaging with ^{111}In-pentetreotide SPECT has an important role in evaluating patients with GEP NETs. Furthermore, multivariate analysis of GEP NETs has revealed significant differences in age, size, depth of invasion, lymph node involvement, distant metastasis, and location. Ito et al. (*9*) reported distant metastases in 21% of patients with nonfunctioning tumors or pancreatic endocrine tumors, occurring more frequently as tumor size increased (>2 cm). Lymph node metastases from gastrointestinal NETs also occurred more frequently as tumor size increased (>1 cm) (*9*).

Received May 14, 2020; revision accepted Jun. 26, 2020.
For correspondence or reprints contact: Takao Kanzaki, Gunma University Hospital, 3-39-15 Showa, Maebashi, 371-8511 Japan. Email: tkanzaki@gunma-u.ac.jp
Published online Sep. 4, 2020.

Optimization of SPECT image reconstruction for the detection of small lesions is crucial to the interpretation of ^{111}In-pentetreotide SPECT images of GEP NETs. The ordered-subset expectation maximization (OSEM) algorithm (subset number and iteration number for a defined number of subsets) (*10*) has become the most important iterative reconstruction technique in SPECT studies. There is no standard technique to optimize the differential correction method for ^{111}In-pentetreotide SPECT imaging of GEP NETs.

The purpose of this study was to determine the optimal correction parameter settings for ^{111}In-pentetreotide SPECT images of GEP NETs.

MATERIALS AND METHODS

Phantom Study

The phantom was initially filled to simulate the quantitative outcome measures of tumor density obtained from the SPECT systems. All SPECT images were reconstructed with iterative techniques including OSEM. For the first phantom study, energy window width (EWW) and OSEM reconstruction conditions were used. We used a SPECT QA phantom (JS-10; Kyoto Kagaku Co., Ltd.) containing 5 hot volumes. The phantom was initially filled at a ratio of 16:1, and background activity was simulated with uniform ^{111}In solutions of 352 and 22 kBq/mL. The diameters of the hot volumes were set at 7, 10, 15, 20, and 30 mm. We examined whether determining the optimum EWW from the typical window locations (set at about 171 and 245 keV) was necessary. We compared results from conventional photopeak 15% and 20% windows using 4 different sets of EWW parameters. In addition, the scheme of optimization of the SPECT images with use of the OSEM technique included 6 different sets of reconstruction parameters. The analysis used the number of subsets (8) and the variable number of iterations (3–8).

For the second phantom study, an anthropomorphic abdominal phantom (LKS [liver/kidney]; Kyoto Kagaku Co., Ltd.) was used for ^{111}In-pentetreotide SPECT imaging. The tumor-to-liver-to-background concentration ratio was 16:4:1, and background activity was simulated with uniform ^{111}In-pentetreotide solutions of 352, 88, and 22 kBq/mL (OctreoScan; Fujifilm Toyama Chemical Co., Ltd.). Because the SPECT QA phantom study showed a 15-mm hot signal, we made a phantom to simulate the tumors using rods 15 mm in diameter. Based on the comparison of 4 correction techniques, the triple energy window was used for scatter correction (SC), whereas CT-based correction was used for AC. Correlation analysis was performed using 4 groups: no correction (NC), SC, AC, and CC (combined SC and AC).

Clinical Study

Twenty patients (13 men and 7 women; age range, 37–81 y) with suspected GEP NET who underwent abdominal ^{111}In-pentetreotide SPECT from April 2017 to April 2019 were selected in a masked manner for enrollment in this retrospective study. Final diagnoses (20 GEP NETs) were confirmed by an endocrine physician as shown in Table 1. The patients were administered 111 MBq of ^{111}In-pentetreotide, and images were acquired 4 h after injection. The patients did not undergo any preparation before scanning.

The study protocol was approved by the Ethics Committee of Gunma University (approval HS 2019-067).

SPECT Acquisition Conditions

An E-CAM (Canon Medical Systems) dual-detector γ-camera system equipped with a medium-energy low-penetration collimator was used for both the phantom study and the clinical study. Patients were scanned at 10° intervals over 360° (36 s/step, 11 min in total) in a supine position using step-and-shoot mode and a 128 × 128 matrix. The reconstructed pixel size was 4.8 × 4.8 mm, with a zoom of 1.0. The energy for ^{111}In was set at 171 keV ± 10% (20%) and 245 keV ± 7.5% (15%). With regard to energy, the resolution was 10.4%. The scattered-radiation-estimate window was set on both sides of the photopeak window at 7% of the window width. Emission data were reconstructed using a GMS-7700R workstation (Canon Medical Systems). Reconstruction was based on the OSEM algorithm (*10*). A Butterworth filter (photopeak image: order of 8, cutoff frequency of 0.50 cycles/cm; Compton scatter image: order of 8, cutoff frequency of 0.4 cycles/cm for SC) was used as a prefilter.

TABLE 1
Patient Characteristics

Characteristic	Data
Age (y)	66.0 ± 15.6 (37–81)
Sex	
Male	13
Female	7
Final diagnosis	
Pancreatic NET	1
Stage G1	7
Stage G2	2
Stage unclear	6
Duodenal NET	2
Rectal NET	2
Lymph node metastases of NET	1

Qualitative data are numbers; continuous data are mean ± SD followed by range (n = 20 patients).

Image Processing

SC was set using triple energy windows (*11*) in which the main window was at the peak of 171 keV ± 10% and 245 keV ± 7.5% and 2 additional windows for SC were at 171 and 245 keV ± 7%. The OSEM CT-based method was used for AC, with the boundary fixed in the abdomen. The AC was $\mu = 0.135\ cm^{-1}$. An automatic registration tool (ART; Canon Medical Systems) was used with the 320-detector CT scanner (Aquilion ONE; Canon Medical Systems) data for AC of the emission images (*12*). This software tool uses 2 methods for automatic registration of 3-dimensional images acquired from different scanners. All CT datasets for ART were acquired within 2 mo from the day on which somatostatin receptor scintigraphy was conducted. We applied OSEM with 8 subsets and 6 iterations in the clinical study. The data were reconstructed into 4 groups to compare the effects of AC and SC: NC, SC, AC, and CC. In the clinical study, NC was taken as a reference, as is common in clinical practice.

Contrast-to-Noise Ratio (CNR) for the SPECT Analysis

All SPECT data were imported into software (Daemon Research Image Processor; Fujifilm Toyama Chemical Co., Ltd.). Using the SPECT QA phantom data, we determined the optimal parameters of EWW based on the image reconstruction method and iterations in the reconstruction. Figure 1 shows an example region of interest (ROI). We evaluated the CNR of the SPECT

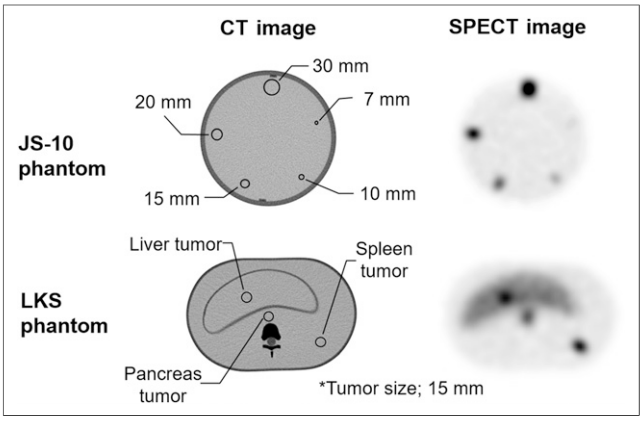

FIGURE 1. Comparison of SPECT QA (JS-10) phantom images for EWW, image reconstruction conditions, and CT images and of anthropomorphic abdominal (LKS) phantom for image collection conditions.

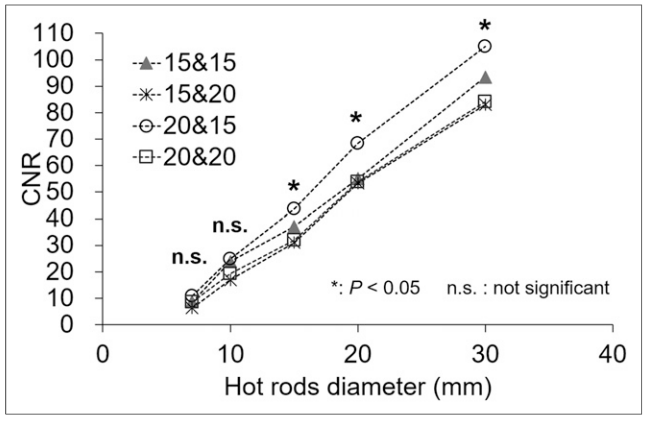

FIGURE 2. CNR of hot rods for optimum EWW in phantom study. EWW setting of 171 keV ± 10% and 245 keV ± 7.5% was significantly better than other settings ($P < 0.05$).

values in 5 circular ROIs corresponding to each rod diameter (7, 10, 15, 20, and 30 mm; Fig. 1). The ROI positioning was based on the CNR method developed by Sreedhar (*13*). The CNR for each sphere in the phantom was calculated as

$$\text{CNR} = |\frac{C - C_B}{\sigma_{BG}}|,$$

where C is the average number of counts in the sphere of interest, C_B is the average number of counts in the background (BG) ROI, and σ_{BG} is the SD in the background ROI. Using LKS phantom data, we determined the optimal parameters for correcting the images. We evaluated the CNR of the SPECT values in 3 circular ROIs (liver, pancreas, and spleen) to produce a phantom simulating a tumor with a rod 15 mm in diameter, as in Figure 1. Similarly, in the clinical study, ROIs were selected in the SPECT images over the tumor (C) and abdomen (C_B, σ_{BG}) at 4 h after injection.

Statistical Analysis

We compare the 4 different sets of reconstruction correction settings for ^{111}In-pentetreotide SPECT imaging. The Tukey test was used in GEP NET patients ($n = 20$). Statistics were performed with IBM SPSS Statistics (version 23; IBM Corp.). A P value of less than 0.05 was considered significant.

RESULTS

Phantom Study

The results of the SPECT QA phantom study were analyzed according to the EWW and OSEM from ^{111}In-pentetreotide SPECT. The ^{111}In-pentetreotide SPECT image reconstruction conditions were compared using the CNR parameter acquired from the SPECT QA phantom.

Figure 2 shows the optimum EWW from all typical window locations (set at about 171 and 245 keV) and 4 different sets of EWW parameters. When the hot-rod diameter was 15, 20, or 30 mm, the CNRs using the energy windows of 171 keV ± 10% and 245 keV ± 7.5% were significantly different from the other parameters ($P < 0.05$).

OSEM reconstruction conditions are plotted as the number of iterations in Figure 3. The numbers of iterations using OSEM reconstruction conditions were also compared on the basis of CNR. The number of subsets was set at 8. The numbers of iterations were compared using different reconstruction parameters. The result showed that the highest CNR for OSEM reconstruction conditions was obtained with 8 subsets and 6 iterations ($P < 0.05$).

Figure 4 shows the OSEM collection conditions obtained by CNR measured for ^{111}In-pentetreotide SPECT. This finding confirmed the LKS phantom study results. When NC, SC, and AC were used, the CNR of the pancreas was significantly lower than that of liver ($P < 0.05$). The representative axial phantom scan slices shown in Figure 5 demonstrate the effects of SC, AC, and CC on the tumor compartment and background.

Clinical Study

Figure 6 shows the CNR results for GEP NET patients evaluated by 4 different methods of correcting ^{111}In-pentetreotide

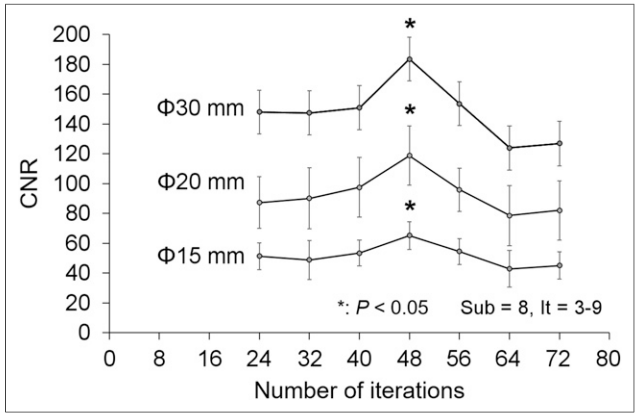

FIGURE 3. Optimization of OSEM technique between CNR and numbers of iterations in phantom study. OSEM reconstruction conditions of 8 subsets and 6 iterations gave significantly highest CNR ($P < 0.05$).

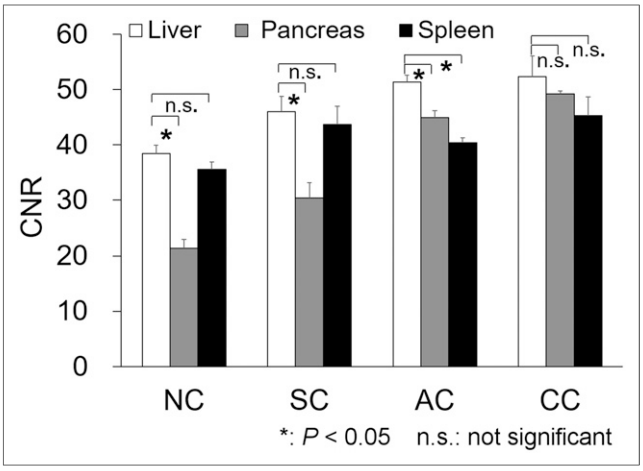

FIGURE 4. Comparison of 4 techniques of SPECT image correction (NC, SC, AC, and CC) in phantom study. Although underestimation occurred in pancreas when NC and SC were used, CC showed no significant difference ($P = 0.83$). In particular, CC gave significantly better CNR for pancreas than did NC or SC ($P < 0.05$).

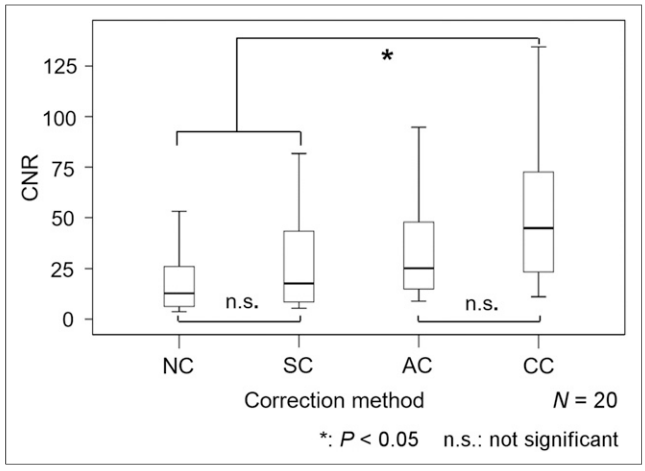

FIGURE 6. Box plot of CNR evaluated by 4 methods (NC, SC, AC, and CC) in 20 GEP NET patients. NC and SC showed no significant difference ($P = 0.86$), whereas CC showed significant differences from NC and SC.

SPECT images. SC and AC did not result in a CNR significantly different from that for NC ($P = 0.86$). Only CC showed a significantly higher CNR than that for NC and SC ($P < 0.05$).

Figure 7 shows a representative case: a 66-y-old woman with a body mass index of 24.8 kg/m^2. A hypervascular pancreatic-head lesion 15 mm in diameter was noted on early dynamic MR images, and postsurgical pathologic examination confirmed it to be a G2 NET. Since the pancreatic head is relatively deep in the abdomen, ^{111}In-pentetreotide SPECT with NC showed weak visualization of the lesion. SPECT with CC better delineated the lesion by the decreasing background noise and AC.

DISCUSSION

On the basis of a phantom study, we determined EWW, OSEM reconstruction conditions (8 subsets and 6 iterations), and correction parameter settings to improve the CNR for ^{111}In-pentetreotide SPECT images. In a clinical study of GEP NET patients, the CNR of the lesion when corrected with CC was significantly higher than that with NC or SC.

The optimal EWW and OSEM reconstruction conditions improved the CNR for ^{111}In-pentetreotide SPECT acquisition. The European Neuroendocrine Tumor Society consensus guidelines—the standard of care in NETs—provide a tool to accurately assess the diagnosis of NETs, recommending that both photopeaks of ^{111}In be centered over 20% energy windows (*14*). In our study, we compared 4

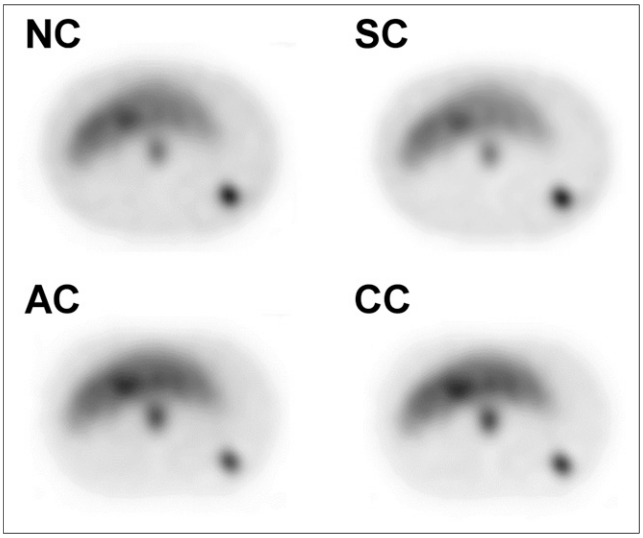

FIGURE 5. Axial phantom SPECT images corrected by 4 methods (NC, SC, AC, and CC).

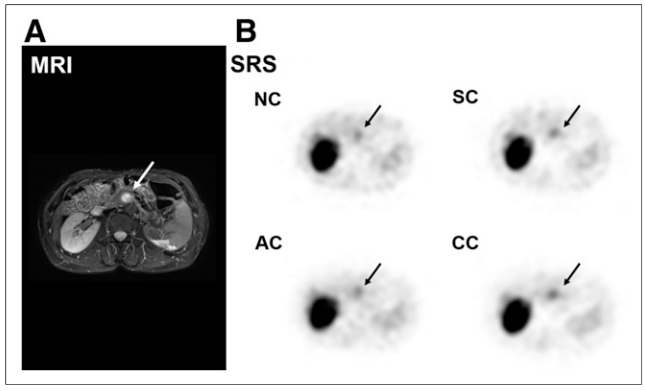

FIGURE 7. Case of G1 NET of pancreatic head without metastasis. (A) Highly enhanced lesion (arrow) in pancreas is noted in early dynamic MR image. (B) ^{111}In-pentetreotide SPECT images with NC, SC, AC, and CC depict abnormal uptake in corresponding upper abdominal area (arrows). Although images with SC and AC show comparable visualization of lesion with NC, CC delineates lesion most clearly.

different sets of EWW parameters based on this guideline. The optimal EWW was found to be 171 keV ± 10% and 245 keV ± 7.5%, compared with the guideline conditions. We thus recommend that the optimal EWW should be set to 171 keV ± 10% and 245 keV ± 7.5% in the clinic. In the OSEM algorithm, an excessive number of iterations might result in SPECT images that are too noisy (*15*).

Alexander et al. reported that somatostatin receptor scintigraphy missed one third of all tumor lesions found by surgery; somatostatin receptor scintigraphy detected 30% of gastrinomas 1.1 cm or smaller, 64% of those 1.1–2 cm, and 96% of those larger than 2 cm (*16*). To minimize false-negative diagnoses, Ruf et al. reported that AC in ^{111}In-pentetreotide SPECT/CT data has the potential to improve sensitivity, especially with a more centrally localized focus (*17*). In our phantom study, CC in the pancreatic area showed a higher CNR than did NC, possibly because of AC and SC. Similar results were obtained in clinical studies (*18–20*).

Improvement of ^{111}In-pentetreotide SPECT diagnosis is needed for small tumors (<2 cm) (*21*). Although comparisons with reference images, such as MRI or CT, is important in this case, careful observation of the ^{111}In-pentetreotide SPECT images is also necessary (*22,23*). Because SPECT/CT is not available at our hospital, we have used AC methods to automate the registration of CT medical images acquired from different modalities. This technique can be applied at any imaging facility equipped with a SPECT scanner. We suggest that institutions without a SPECT/CT scanner consider the optimal parameters for SPECT practice.

Our study had several limitations. The phantom study set the tumor and background radioactivity to 16:1. Radioactivity may not be supported in all clinical cases. Optimization of EWW may not be enough to allow consideration of only 2 window widths—20% and 15%—of photopeak energy. A variety of EWWs should be compared. We have evaluated the optimal parameters for SPECT (E-CAM) practice. However, in other institutions, different SPECT devices may not be exactly compatible or support the same parameters. As a part of quality control, each center must check the optimal correction settings of its own SPECT device. The number of patients was small. Evaluation of a larger number of patients should be considered. Moreover, as the study was retrospective, differences in the types of NETs and distribution of the lesions could not be controlled. A greater variety of patients, based on grade, age, and location of lesions, should be compared in a future study.

CONCLUSION

AC and SC of ^{111}In-pentetreotide SPECT can improve GEP NET imaging, with better contrast and sharper lesion delineation than is possible with conventional SPECT imaging. In patients with GEP NETs, optimal setting of SPECT parameters can improve the diagnostic accuracy of SPECT images and therefore may lead to better-informed treatments.

DISCLOSURE

No potential conflict of interest relevant to this article was reported.

REFERENCES

1. Yao JC, Hassan M, Phan A, et al. One hundred years after "carcinoid": epidemiology of and prognostic factors for neuroendocrine tumors in 35,825 cases in the United States. *J Clin Oncol.* 2008;26:3063–3072.
2. Ito T, Igarashi H, Jensen RT. Therapy of metastatic pancreatic neuroendocrine tumors (pNETs): recent insights and advances. *J Gastroenterol.* 2012;47:941–960.
3. Ito T, Lee L, Hijioka M, et al. The up-to-date review of epidemiological pancreatic neuroendocrine tumors in Japan. *J Hepatobiliary Pancreat Sci.* 2015;22:574–577.
4. Lloyd RV, Osamura RY, Klöppel G, Rosai J. *WHO Classification of Tumours of Endocrine Organs*. 4th ed. IARC Press; 2017.
5. Oberg K. State of the art and future prospects in the management of neuroendocrine tumors. *Q J Nucl Med.* 2000;44:3–12.
6. Sharma P, Singh H, Bal C, Kumar R. PET/CT imaging of neuroendocrine tumors with ^{68}gallium-labeled somatostatin analogues: an overview and single institutional experience from India. *Indian J Nucl Med.* 2014;29:2–12.
7. Schillaci O, Spanu A, Scopinaro F, et al. Somatostatin receptor scintigraphy in liver metastasis detection from gastroenteropancreatic neuroendocrine tumors. *J Nucl Med.* 2003;44:359–368.
8. Volterrani D, Orsini F, Chiacchio S. Multiagent targeting of neuroendocrine neoplasms. *Clin Transl Imaging.* 2013;1:407–421.
9. Ito T, Sasano H, Tanaka M, et al. Epidemiological study of gastroenteropancreatic neuroendocrine tumors in Japan. *J Gastroenterol.* 2010;45:234–243.
10. Hudson HM, Larkin RS. Accelerated image reconstruction using ordered subsets of projection data. *IEEE Trans Med Imaging.* 1994;13:601–609.
11. Ogawa K. Simulation study of triple-energy-window scatter correction in combined Tl-201, Tc-99m SPECT. *Ann Nucl Med.* 1994;8:277–281.
12. Motomura N, Takahashi M, Nakagawara G, Iida H. Evaluation of a SPECT attenuation correction method using CT data registered with automatic registration software. *IEEE Nucl Sci Symp Conf Rec.* 2003;4:2676–2680.
13. Sreedhar K. Enhancement of images using morphological transformations. *Int J Comput Sci Inf Technol.* 2012;4:33–50.
14. Kwekkeboom DJ, Krenning EP, Scheidhauer K, et al. ENETS consensus guidelines for the standards of care in neuroendocrine tumors: somatostatin receptor imaging with III In-pentetreotide. *Neuroendocrinology.* 2009;90:184–189.
15. Gutman F, Gardin I, Delahaye N, et al. Optimisation of the OS-EM algorithm and comparison with FBP for image reconstruction on a dual-head camera: a phantom and clinical ^{18}F-FDG study. *Eur J Nucl Med Mol Imaging.* 2003;30:1510–1519.
16. Alexander HR, Fraker DL, Norton JA, et al. Prospective study of somatostatin receptor scintigraphy and its effect on operative outcome in patients with Zollinger-Ellison syndrome. *Ann Surg.* 1998;228:228–238.
17. Ruf J, Steffen I, Mehl S, et al. Influence of attenuation correction by integrated low-dose CT on somatostatin receptor SPECT. *Nucl Med Commun.* 2007;28:782–788.
18. Ljungberg M, Strand SE. Attenuation and scatter correction in SPECT for sources in a nonhomogeneous object: a Monte Carlo study. *J Nucl Med.* 1991;32:1278–1284.
19. Hutton BF, Buvat I, Beekman FJ. Review and current status of SPECT scatter correction. *Phys Med Biol.* 2011;56:R85–R112.
20. Rahmim A, Zaidi H. PET versus SPECT: strengths, limitations and challenges. *Nucl Med Commun.* 2008;29:193–207.
21. Delle Fave G, O'Toole D, Sundin A, et al. ENETS consensus guidelines update for gastroduodenal neuroendocrine neoplasms. *Neuroendocrinology.* 2016;103:119–124.
22. Reznek RH. CT/MRI of neuroendocrine tumours. *Cancer Imaging.* 2006;6(suppl):S163–S177.
23. Dromain C, Déandréis D, Scoazec JY, et al. Imaging of neuroendocrine tumors of the pancreas. *Diagn Interv Imaging.* 2016;97:1241–1257.